

Challenges in Batch-to-Bed Translation Involving Inflammation-Targeting Compounds in Chronic Epilepsy: The Case of Cathepsin Activity-Based Probes

Roa'a Hamed, Emmanuelle Merquioli, Ivan Zlotver, Galia Blum, Sara Eyal,^{*,ll} and Dana Ekstein^{*,ll}



Cite This: *ACS Omega* 2024, 9, 6965–6975



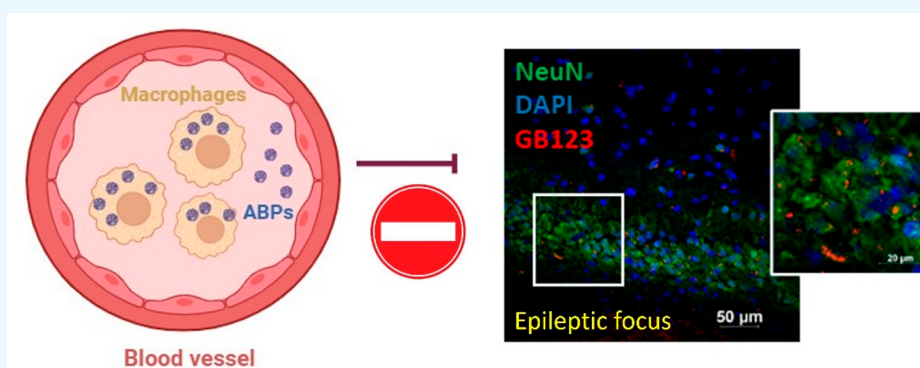
Read Online

ACCESS |

Metrics & More

Article Recommendations

Supporting Information



ABSTRACT: Our goal was to test the feasibility of a new theranostic strategy in chronic epilepsy by targeting cathepsin function using novel cathepsin activity-based probes (ABPs). We assessed the biodistribution of fluorescent cathepsin ABPs *in vivo*, *in vitro*, and *ex vivo*, in rodents with pilocarpine-induced chronic epilepsy and naïve controls, in human epileptic tissue, and in the myeloid cell lines RAW 264.7 (monocytes) and BV2 (microglia). Distribution and localization of ABPs were studied by fluorescence scanning, immunoblotting, microscopy, and cross-section staining in anesthetized animals, in their harvested organs, in brain tissue slices, and *in vitro*. Blood–brain-barrier (BBB) efflux transport was evaluated in transporter-overexpressing MDCK cells and using an ATPase activation assay. Although the *in vivo* biodistribution of ABPs to both naïve and epileptic hippocampi was negligible, *ex vivo* ABPs bound cathepsins preferentially within epileptogenic brain tissue and colocalized with neuronal but not myeloid cell markers. Thus, our cathepsin ABPs are less likely to be of major clinical value in the diagnosis of chronic epilepsy, but they may prove to be of value in intraoperative settings and in CNS conditions with leakier BBB or higher cathepsin activity, such as status epilepticus.

INTRODUCTION

Epilepsy is a common debilitating brain disease and, despite adequate treatment with antiseizure medications (ASMs), about one-third of the patients will continue to have seizures.^{1,2} Moreover, no ASM on the market cures epilepsy or modifies epileptogenesis, and the majority of drugs primarily target neuronal activity.³ Over the past decade, there have been attempts to develop or repurpose immune modulators for treating epilepsy. Whereas in the acute setting of refractory status epilepticus there is a therapeutic value of compounds such as rituximab,⁴ trials of using similar drugs to treat chronic epilepsy⁵ or to prevent epileptogenesis⁶ have not achieved efficacy end points. Therefore, there is a need for a better understanding of the immune pathways that contribute to the development of epilepsy and seizure perpetuation, which will ultimately lead to the identification of new therapeutic targets.

Cysteine cathepsins are a group of proteases critically involved in the function of myeloid cells (macrophages and

microglia).^{7,8} Elevated cathepsin levels and activity have been implicated in cardiovascular, neurological, and other diseases,^{7,9–11} and cathepsins secreted by activated microglia were shown to induce neuronal death.^{12,13} Loss of cathepsin B inhibition and increased activity of cathepsins B, L, and S in lymphoblastoid cells were reported in patients with the most common type of progressive myoclonus epilepsy (EPM1).^{14,15} Cathepsins S, B, and D were detected within myeloid cells and astrocytes in murine hippocampi, during the first 12 days after kainate-induced status epilepticus.^{16,17} However, cathepsin activity has not been assessed in the models of chronic

Received: November 4, 2023

Revised: December 13, 2023

Accepted: December 14, 2023

Published: February 1, 2024



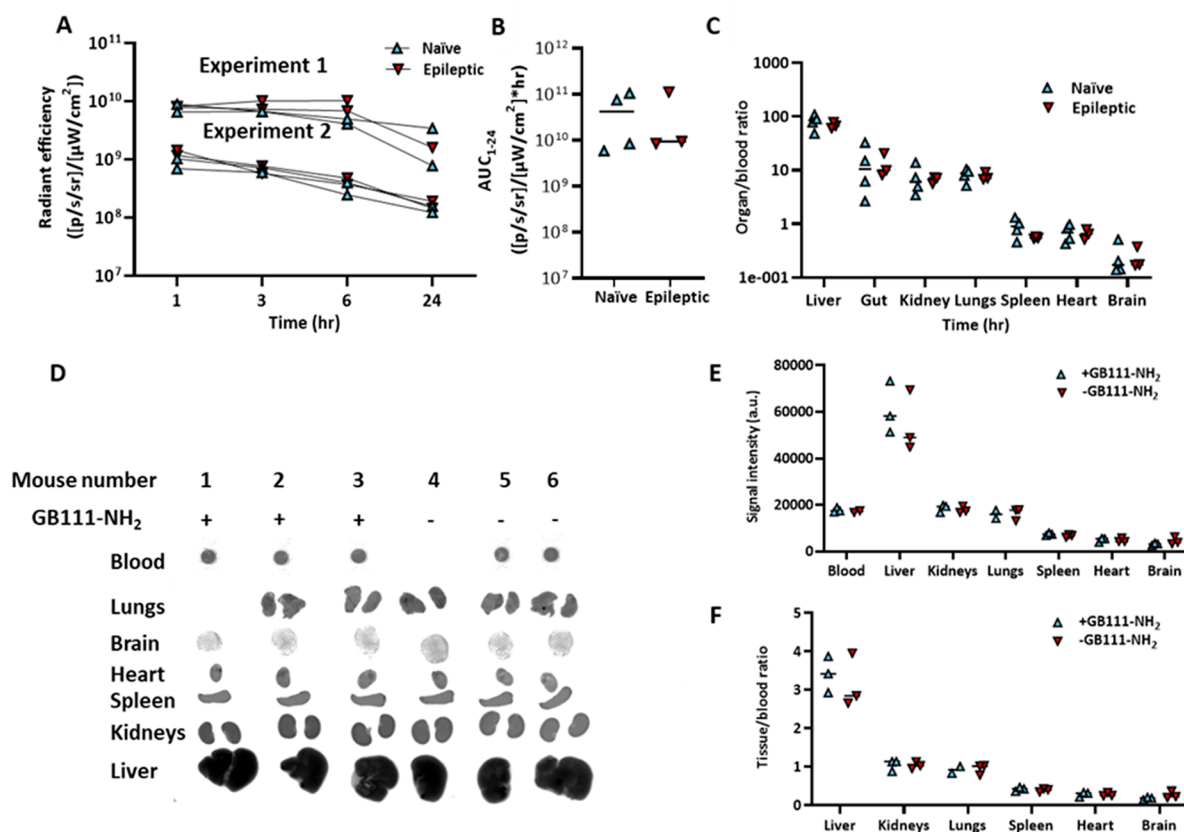


Figure 1. GB123 poorly distributes into naïve and epileptic mice brains. GB123 distribution in epileptic and naïve mice: (A) timeline of GB123 signal in the mice feet; (B) AUC analysis for GB123 in epileptic and naïve mice; (C) ex vivo analysis of GB123 fluorescence (normalized by individual blood fluorescence). (D) Typhoon FLA 9500 scans of tissues from naïve mice 24 h after GB123 injection. The left three columns represent organs obtained from mice pretreated with the cathepsin inhibitor GB111-NH₂. (E, F) Quantifications of these findings (absolute values and values corrected to blood concentrations). Although some differences between inhibitor-pretreated and not pretreated values were observed (most pronounced in the brains), the inhibitor did not considerably or statistically significantly affect GB123 distribution, suggesting mostly nonspecific accumulation.

epilepsy. Recently we have shown that cathepsin inhibition can lead to macrophage cell death.^{8,9} Because activated microglia are involved in the pathophysiology of epilepsy, it is plausible that cathepsin inhibitors might modulate seizures and that the binding of labeled cathepsin–ligands may be utilized for imaging of epileptogenic brain tissue.

We hypothesized that cathepsins within myeloid cells in epileptic tissue are especially active and can therefore be exploited to develop a novel theranostic approach for detecting epileptogenic brain areas and potentially preventing seizures. Our goal was therefore to study cathepsin function in chronic focal epilepsy using a rodent model of hippocampal epilepsy. To accomplish it, we applied fluorescent activity-based probes (ABPs) we developed, which selectively bind active cathepsin B, L, and S:^{11,18–20} a cathepsin inhibitor (GB111-NH₂),¹⁹ quenched (GB137), and nonquenched (GB123) cathepsin ABPs that covalently bind to the target proteases, allowing biochemical analysis of the respective enzymes.

RESULTS

Systemic In Vivo Distribution of GB123 in Naïve and Epileptic Mice. In this series of experiments, the distribution of GB123 into various organs after intravenous injection to naïve and epileptic mice was documented. The GB123 signal decayed slowly (Figure 1A and Supporting Information Figure S1A,D), suggesting prolonged retention in blood and foot

tissues, with similar kinetics in epileptic and naïve mice (Figure 1A,B). Ex vivo analysis of harvested organs showed the lowest intensity in the brain (Figure 1C). To further characterize the tissue distribution of i.v.-administered GB123, we injected the probe into six naïve mice and harvested their organs for fluorescence identification ex vivo (Figure 1D). Three of the mice were pretreated with the nonfluorescent cathepsin inhibitor GB111-NH₂, to test the specific binding of GB123 to cathepsins, as suggested by differences in the fluorescence between inhibitor pretreated and not pretreated samples. The inhibitor only scarcely affected the tissue fluorescence (Figure 1E,F), implying that GB123 has not cleared from the tissues and still can be detected even if it is unbound to cathepsins.

In Vivo Administered Cathepsin ABPs Do Not Label Epileptogenic Hippocampus. Since the fraction of the dose which crosses the BBB may be minor even for CNS-active drugs,²¹ we further characterized the brain distribution of in vivo administered GB123. As expected, there were more microglia (Iba1 staining, middle panels) in the epileptic brain than in the naïve brain (Figure 2). However, no cathepsin activity could be observed in the brains (right panels), indicating that the in vivo administered probe did not stain the epileptic focus.

ABPs Specifically Bind to Rodent and Human Brain Tissue Ex Vivo. While GB123 did not bind to brain tissue following its systemic administration to mice in vivo (Figure

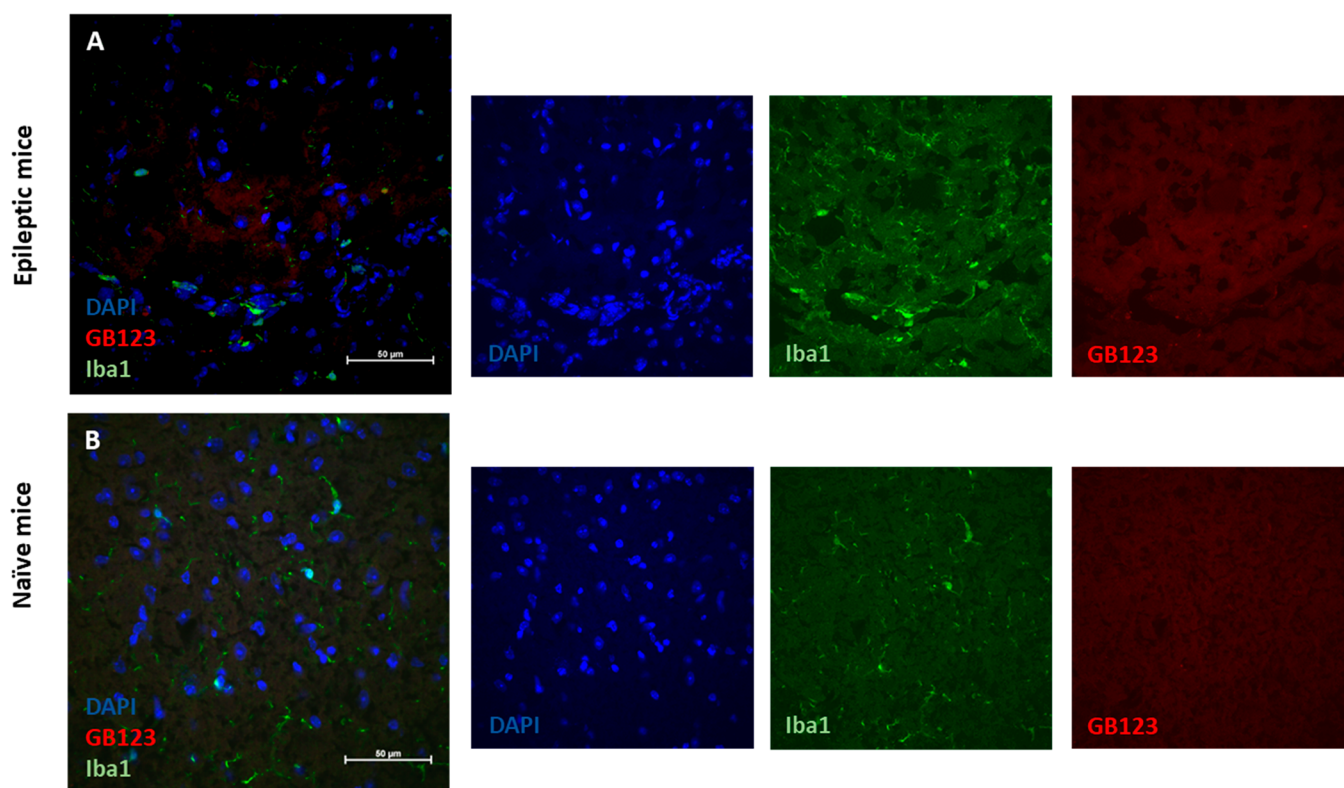


Figure 2. Lack of detection of in vivo injected GB123 in epileptogenic and naïve brain tissue. Detection of GB123 signal in red in epileptic mouse brain tissue (A) and naïve mouse brain (B) stained with macrophage marker (Iba1) in green and nuclear staining (DAPI) in blue.

3A, left panel), ex vivo incubation of GB123 with extracts from the same mice resulted in clear specific binding to brain cathepsin proteases (Figure 3A, right panel, mice 1, 5 and 1–6, respectively). The ex vivo but not in vivo pretreatment with GB111-NH₂ blocked GB123 binding (Figure 3A). Ex vivo GB137 also bound to rat brain tissue, significantly more to the epileptic than the naïve brains (Figure 3B–E,J). Similarly, GB137 labeled cells in specimens from human epileptic tissue were resected during epilepsy surgery (Figure 3F–I). Labeling was significantly inhibited by GB111-NH₂ (Figure 3K), suggesting specific binding of the GB compounds to active cathepsins in the tissue and elevation of the cathepsin activity in the epileptic brain.

GB123 is Not a Substrate of Efflux Transporters at the BBB. The cerebral distribution of many drugs is limited by two major transporters which are localized at the BBB: the multidrug resistance transporter 1 (MDR1; P-gp) and the breast cancer resistance protein (BCRP).^{3,22} Accordingly, we characterized the interaction of GB123 with these transporters to decipher the ex vivo–in vivo discrepancy. We found that P-gp overexpression and inhibition were associated with a statistically significant but not clinically meaningful change (<2-fold)²³ in the cellular accumulation of GB123 (Figure 4A,B). In addition, GB123 staining was comparable across all cell types, despite clear overexpression of P-gp and BCRP in the respective cell lines (Figure 4C,D). In line with those results, GB123 did not activate the respective transporter ATPases (Figure 4E,F). These experiments demonstrate that GB123 is not a good substrate for P-gp or BCRP.

Cellular Localization of GB123 within the Epileptic Mouse Hippocampus. We further characterized the regional GB123 binding in the epileptogenic brain, focusing on the

hippocampus: dentate gyrus (DG) region and CA3 and CA1 regions. The GB123 signal was exclusively detected in all areas of the epileptic (Figure 5 and Supporting Information Figure S2) but not in the naïve hippocampi (Figure S2). Cathepsin activity was not detected in Iba1-positive (myeloid) cells (Figure 5A–C), but it was clearly seen in neurons across all of the hippocampal regions (Figure 5D–F).

GB123 is Internalized by Myeloid Cells, in a Time- and Activity-Dependent Manner. Although GB123 did not label myeloid cells ex vivo, it was taken into RAW 264.7 and BV2 cells in a time-dependent manner, and an inflammation-inducing agent increased its uptake (Figure 6). This analysis excluded the insufficient distribution of GB123 into monocytes and microglia as a cause of the poor brain tissue signal.

DISCUSSION

Monocytes are detectable in the human and rat epileptic hippocampi,²⁴ and reducing their recruitment into the brain after status epilepticus was associated with accelerating weight regain, and with attenuation of BBB and neuronal damage.²⁵ Here, we evaluated in a chronic model of epilepsy the potential for clinical use of novel ABPs that target cathepsins within myeloid cells. Although we detected only modest GB123 distribution into the hippocampus ex vivo and negligible hippocampal binding in vivo, our experiments yielded several interesting findings, some of which require further exploration.

The first finding is the modest ability of compounds, which avidly bind a target within monocyte-like cells, to label epileptogenic brain tissue in chronic epilepsy ex vivo. This result is in line with lower cerebral monocyte invasion and glial activation during chronic epilepsy as compared to epileptogenesis.²⁶ Microglial or monocytic GB123 uptake was even less

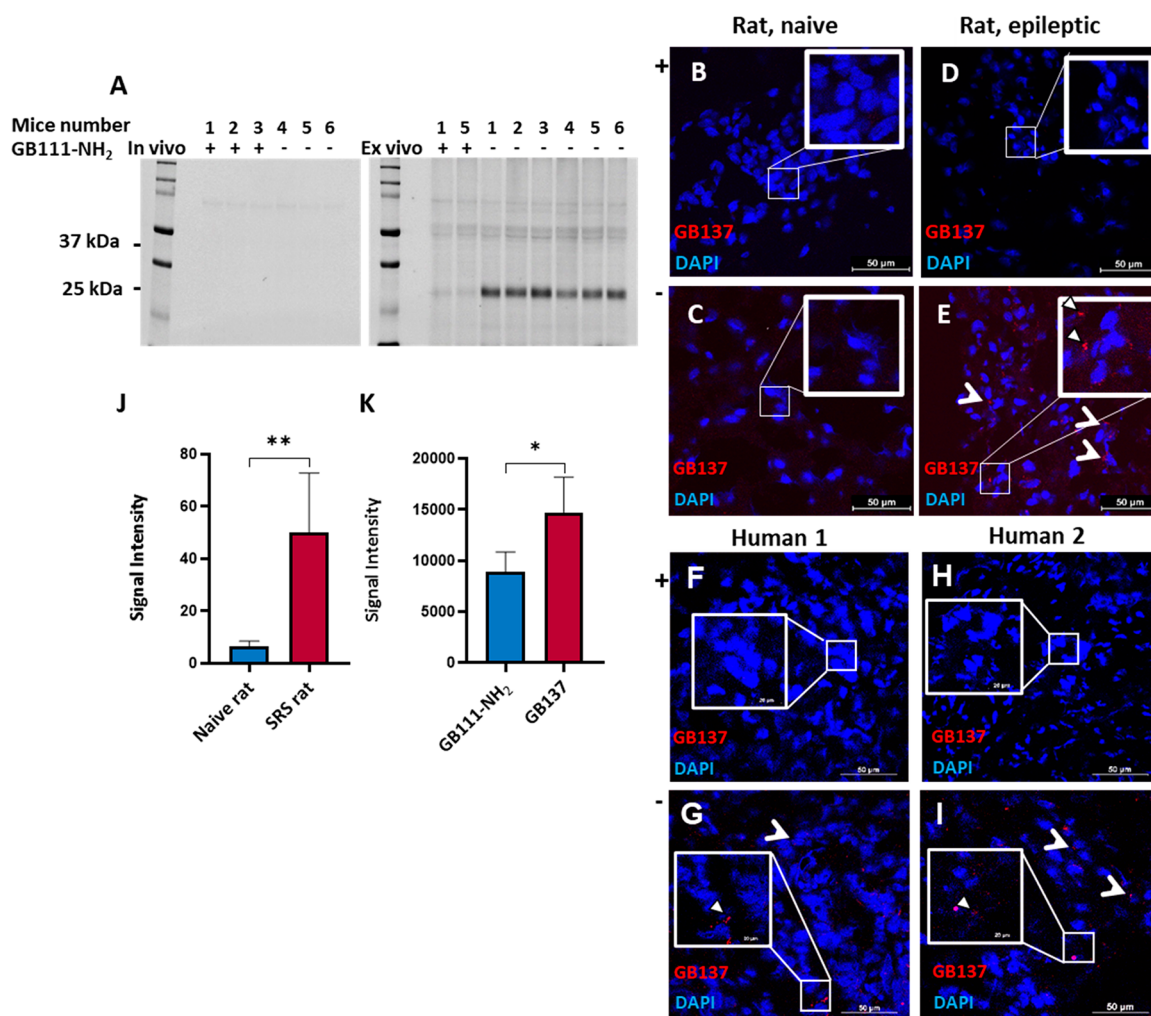


Figure 3. GB123 and GB137, label cathepsins in epileptogenic brain tissue ex vivo. (A) Brain tissues from naïve mice, resected and lysed after pretreatment (lanes 1, 3–5) or not (lanes 4–6) with the nonfluorescent cathepsin inhibitor GB111-NH₂. The lysed proteins were further incubated in vitro with either the GB111-NH₂ (5 μ M; lanes 1 and 2) or the vehicle for 30 min and then with the fluorescent activity-based probe GB123 (2 μ M) for 90 min (right side samples). Equal amounts of protein were separated on gel and scanned for fluorescence. These experiments demonstrated ex vivo but not in vivo cathepsin labeling and inhibition in the mouse brain. GB137 application ex vivo to samples, specifically binding to cathepsins in epileptogenic and naïve brain tissue from rats. Shown are hippocampal cryosections from 2 naïve rats (B, C), and 2 rats with chronic epilepsy (D, E). Sections were stained with DAPI (blue) and incubated with GB137 (red), with (+; B, D) or without (-; C, E) preincubation with GB111-NH₂. Digitally magnified details are presented in the inlets, and the GB137 signal is marked by arrow heads. GB137, applied ex vivo, labeling cells in human epileptogenic brain tissue. Brain sections obtained during neurosurgical resection from patient 1 (F, G) and patient 2 (H, I) were stained with (+; F, H) or without (-; G, I) preincubation with GB111-NH₂ and imaged as per rat brains. (J) Quantification of naïve and epileptic brain rat tissue treated ex vivo with GB137. (K) Quantification of two human brain tissues pretreated ex vivo with or without GB111-NH₂. Statistical analysis was performed using the Mann–Whitney test for rat and human brain tissue. * $p < 0.05$; ** $p < 0.01$. #GB137 is a quenched cathepsin ABP, with very high specificity for cathepsins, used by us in proof-of-concept experiments in rat and human tissue. Follow-up experiments were performed with the unquenched GB123 ABP, since the ex vivo results were similar and its production in large quantities is more readily performed (see [Methods](#) for more information).

pronounced when the compound was administered systemically. Restriction of this compound from the brain was not related to efflux transport because P-gp and BCRP affected the cellular kinetics of GB123 only marginally.

We recently reported that the structural features of ASMs are particularly restrictive and that compounds larger than 400 Da, such as the active XV-765 metabolite VRT-043198 (MW 480 Da), have never made it to the market.²⁷ GB123 (MW 1213 Da) largely deviates from the features we described for compounds that can enter the epileptogenic brain, suggesting that if GB123 labeling was abundant, this could have indicated the existence of disrupted BBB, monocyte infiltration, or both.²⁷ Our current findings imply that neither process takes

place in chronic epilepsy at a sufficient extent to allow pronounced cerebral distribution of GB123, at least in the pilocarpine model. The situation might be different during status epilepticus, when monocytes are more extensively recruited to the brain.²³ Yet, we are not aware of large molecular weight compounds directed against targets protected by the BBB which have demonstrated efficacy in the treatment of status epilepticus.

Our analyses clearly showed that the limited cathepsin labeling is not due to the inability of GB123 to be taken up by monocytes and microglia, lack of inflammation, or inability to bind cathepsins within epileptogenic brain tissue. One suggested explanation is the lower cathepsin activity in

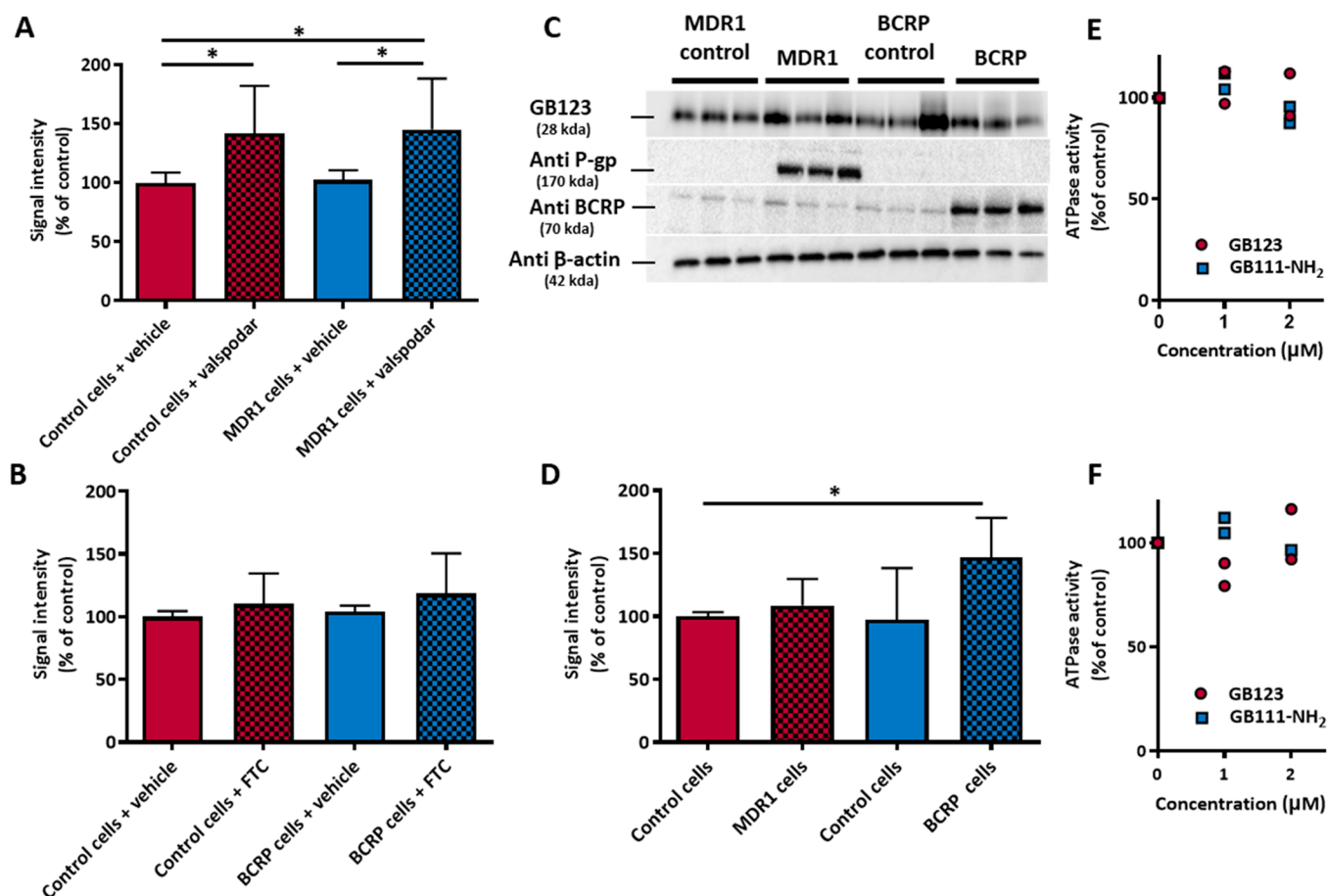


Figure 4. GB123 not a P-gp or BCRP substrate. P-gp (A) and BCRP (B) not affecting the cellular accumulation of GB123. GB123 (1 μM) emission was assessed in MDCK cells by overexpressing P-gp or BCRP (MDCK-MDR1 and MDCK-BCRP, respectively) and in their respective controls, in the presence or absence of respective transporter inhibitors (1.65 μM valsopodar and 10 μM fumitremorgin C—FTC; means \pm SD; $n = 6/\text{group}$). Similar findings were obtained with 2 μM GB123. Results are normalized to the emission intensity of GB123 in vehicle-treated control cells. P-gp, BCRP and β -actin expression (C) and β -actin-normalized GB123 signal in transporter-overexpressing cells in the same samples (D). The cells were exposed to GB123 for 6 h, then harvested, and lysed. Crude lysates were subjected to gel electrophoresis. Following measurement of GB123 fluorescence, proteins were blotted, and transporter expression was measured using primary anti-MDR1 and anti-BCRP antibodies (means \pm SD; $n = 5/\text{group}$). P-gp (E) and BCRP (F) ATPase activity. P-gp or BCRP membranes were incubated with ATP and GB123 or GB111-NH₂, as well as with established MDR1 and BCRP activators (verapamil and sulfasalazine, respectively; positive controls) and sodium orthovanadate (ATPase inhibitor). The product concentration was measured by a reaction. Values represent the mean \pm SD of individual experiments in duplicates. Each data point represents the average of 2 experiments ($n = 4/\text{point}$). Shown are the control-normalized values.

microglia as compared to tumor associated macrophages, which were successfully labeled by us in vivo.^{8,18}

Although our primary aim was to explore cathepsins as possible targets of immune modulation, GB123 exclusively labeled neurons within the brain. Cathepsin B is especially abundant in the human brain during all stages of development¹⁸ and in the cortical and hippocampal neurons in mice.¹⁹ Due to preserved activity in a wide range of pH values,²⁸ its leak from the lysosomes has been implicated in the pathophysiology of neurodegeneration⁷ and of vasculature damage,²⁹ and the need for effective inhibition of cathepsin B to treat neurological diseases has been raised.⁷ Cathepsin B deficiency was associated with favorable outcomes in an animal model of Alzheimer's disease.³⁰ However, inhibition of the same cathepsin was also associated with increased neurodegeneration, contributing to Alzheimer's disease pathology.³¹ These reports imply an important role for lysosomal cathepsin B in the degradation of pathologic proteins, suggesting the need for complex and careful regulation of its activity in

various cellular and extracellular compartments rather than favoring its complete inhibition.

Limitations and Strength. One limitation of the current study is the lack of data on the uptake of GB123 into monocytes in vivo. Yet the extensive distribution into other components of the reticuloendothelial system (primarily the liver) and previous rodent studies suggest this is the case. In addition, the number of animals is limited. However, the results, particularly those obtained ex vivo, are highly consistent, and their nature did not justify the use of larger animal numbers. Also, our results may be limited to the model of epilepsy that we used. This study's strengths include using all possible controls to exclude false negative findings—particularly brain tissue from three species, including humans. Another key strength is our ability to compare the findings to those previously obtained with the same compounds in systemic diseases. Future studies could further explore cathepsin activity in chronic epilepsy, using various methods to quantify cathepsin expression and possibly improving ABPs binding to those molecules.

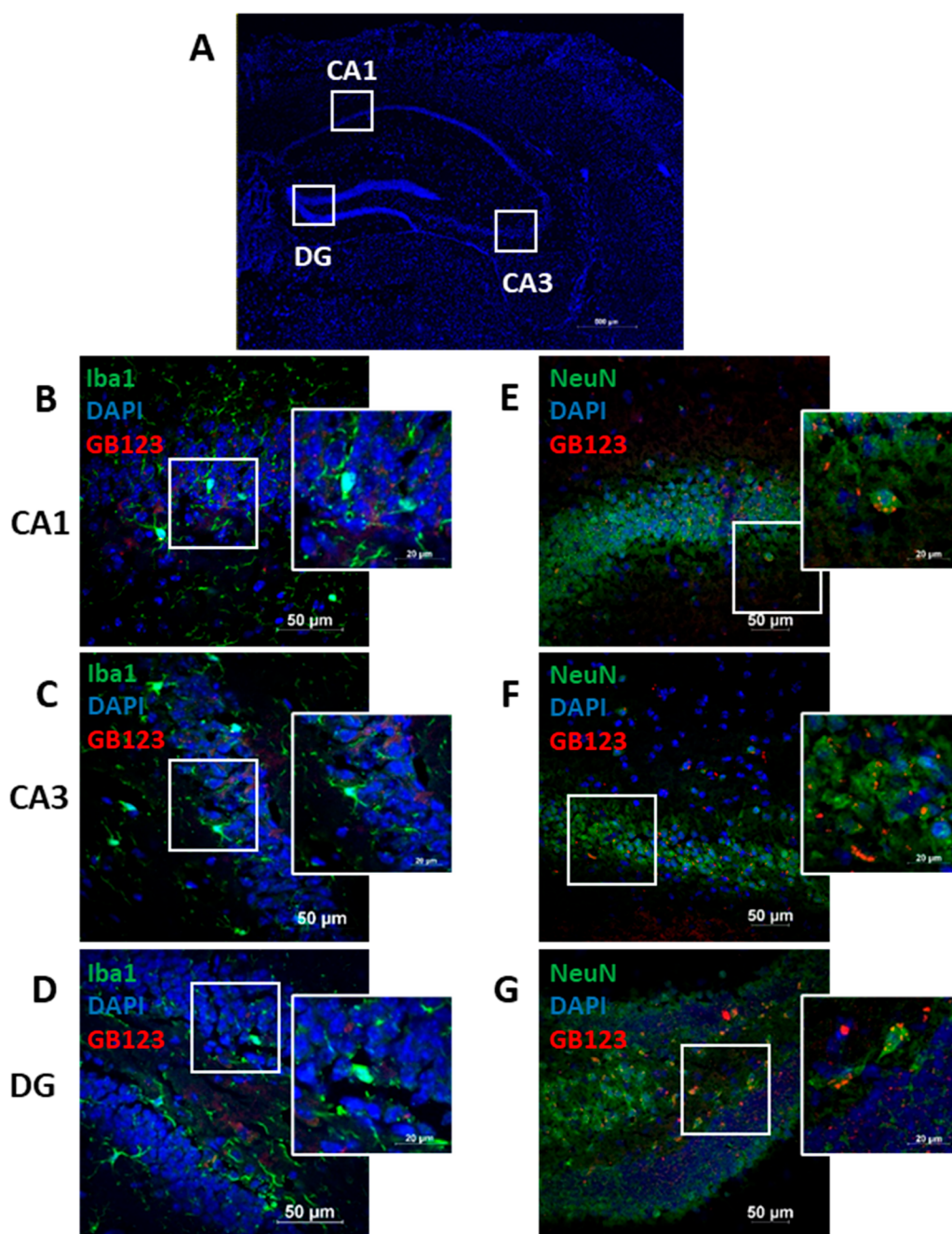


Figure 5. Detection of cathepsins in neuronal cells in epileptogenic brain tissue. (A) DAPI-stained hippocampus at low magnification. The boxed regions (depicted at higher magnification in panels B–G) are in the dentel gyrus (DG), CA1, and CA3 regions of the hippocampus. (B–D) Cathepsin activity labeled by GB123 (red) is not detectable in microglia cells (Iba1 staining) within DG (A), CA1 (B) and CA3 (C) regions of epileptic mice brain after ex vivo staining with GB123 (0.25 μ M for 1 h). (E–G) Cathepsin activity labeled with GB123 (red) detected within the lysosomes of neurons (NeuN staining) (co-staining with NeuN). Confocal microscope images were taken with 60 \times magnification. The boxed areas are digitally enlarged images.

Potential translational value. Our findings suggest that cathepsin-binding ligands would be less preferable as targets for in vivo imaging in epilepsy, in contrast to their potential theranostic applicability in peripheral diseases,^{11–13,27} implying that drug repurposing should be conducted after comparative assessment of the relative functionality of the target in epilepsy versus the condition for which the molecule has been used. For molecules aimed to distribute across the BBB, no assumptions should be made regarding a better distribution across a dysfunctional BBB, at least in chronic epilepsy. More generally,

we support following a robust and thorough paradigm of preclinical assessment of chemical, pharmacokinetic, and pharmacodynamic characterization of investigational agents, even during drug repurposing. Still, future studies may demonstrate a role for cathepsin ABPs in the intrasurgical delineation of epileptogenic tissue and in conditions associated with a leakier BBB or with more intense cathepsin activity, such as status epilepticus. Furthermore, in vivo targeting efficiency of cathepsin ABP could be improved by attenuation of BBB.

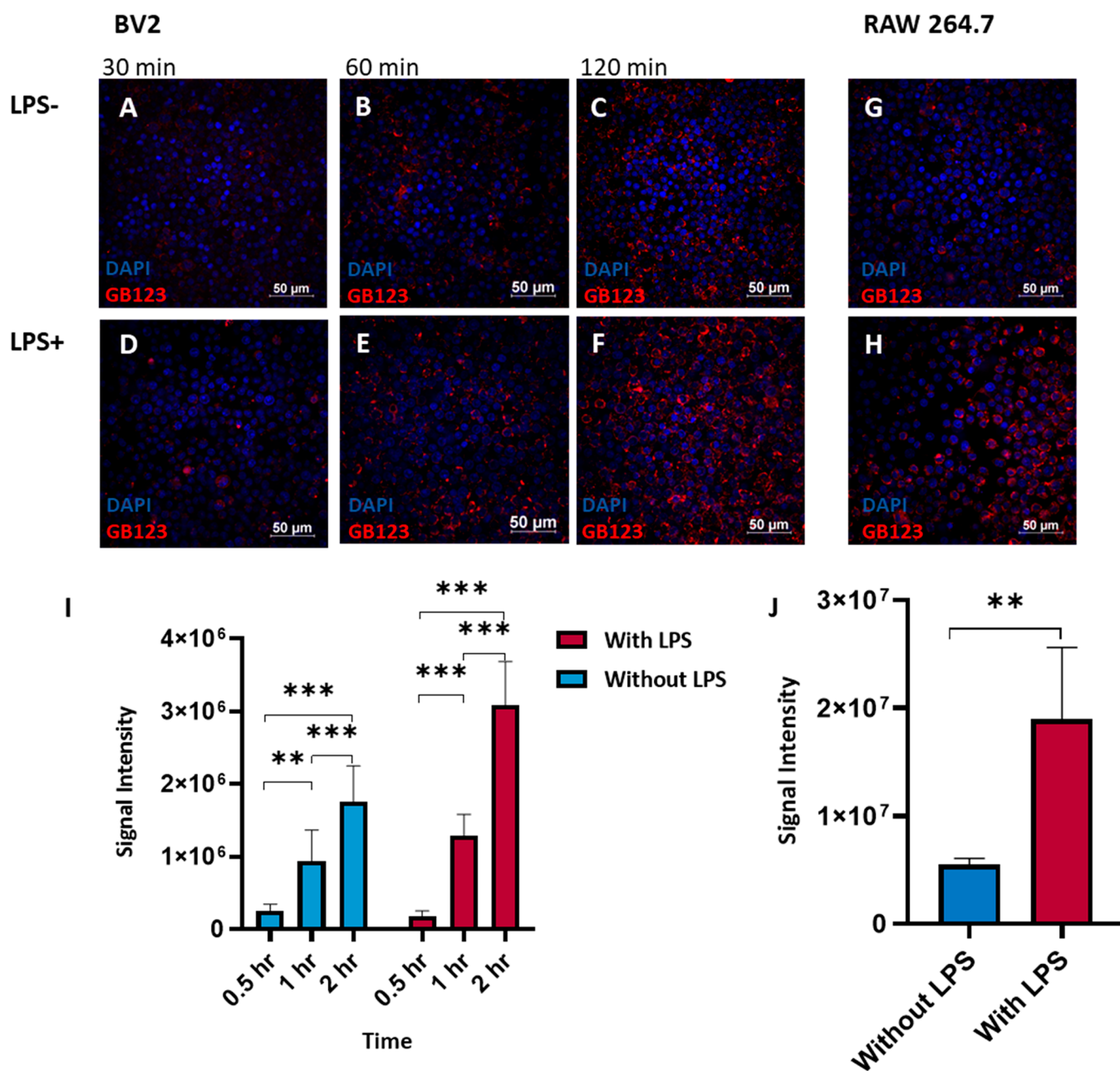


Figure 6. GB123 rapidly taken up by myeloid cells. BV2 cells (DAPI nuclear staining in blue) displaying fluorescent GB123 uptake in red, with or without LPS, at three-time points: 30 min (A, D), 60 min (B, E), and 120 min (C, F). RAW 264.7 cells (DAPI nuclear staining in blue) with and without 2 h incubation with LPS display fluorescent GB123 uptake (G, H), respectively. I, J. Quantification of GB123 signal intensity in BV2 and RAW 264.7 cell lines, respectively, relative to the background (Supplemental Figure 3). $n = 6$ in each experimental group. Statistical analyses were performed using the Mann–Whitney test for RAW 264.7 cell line result, $**p < 0.005$. Tukey's multiple comparison test for BV2 cell line results, $**p < 0.005$ and $***p < 0.0001$.

CONCLUSIONS

Cathepsin ABPs specifically but modestly bound to active cathepsins in brain tissue ex vivo, whereas their in vivo distribution into the epileptogenic hippocampus was poor.

METHODS

Materials. Fluorescent GB123 and GB137 probes and nonfluorescent cathepsin inhibitor GB111-NH₂ were synthesized as described previously.²⁰ The activation of P-gp and BCRP ATPases was measured using the MDR1 and BCRP ATPase assay kits, respectively, as we described before.³² All

standard materials used are listed in the Supporting Information.

Cell Cultures. RAW 264.7 murine monocytes (from Prof. Boaz Tirosch, The Hebrew University) were grown in RPMI 1640 medium supplemented with 10% fetal bovine serum, 2 mM L-glutamine, sodium pyruvate, non-essential amino acids, 100 U/mL penicillin, and 100 μg/mL streptomycin at 37 °C in a 5% CO₂ incubator. BV2 murine microglia cells (from Prof. Sigal Fleisher-Berkovich, Ben-Gurion University) were grown in DMEM supplemented with 10% fetal bovine serum, 2 mM L-glutamine, 100 U/mL penicillin, and 100 μg/mL streptomycin.

Madin–Darby canine kidney (MDCK) II cells transfected with MDR1-coding cDNA (MDCK-MDR1 cells) and parent (MDCK-CT) controls were provided by Dr. Alfred Schinkel (The Netherlands Cancer Institute) and were maintained in Dulbecco's modified Eagle's phenol-free low-glucose medium (DMEM) supplemented with 10% fetal bovine serum, 2 mM L-glutamine, 100 units/mL penicillin, and 100 μ g/mL streptomycin at 37 °C in a 5% CO₂ incubator. MDCK cells transfected with cDNA coding for wild-type BCRP (MDCK-BCRP cells) and cells transfected with pcDNA empty vector (MDCK-vector) were a gift from Dr. Qingcheng Mao (University of Washington). They were grown under similar conditions, except that the medium was Eagle's minimum essential medium (MEM) and cells were additionally supplemented with gentamicin 0.05 mg/mL. The cells were harvested by trypsin–EDTA after achieving 80–90% confluence.

GB123 Uptake into Myeloid Cells In Vitro. RAW 264.7 (1×10^4 cells) or BV2 (1×10^4 cells) cells were cultured in 8-well live-cell microscopy chambers and allowed to adhere to the bottom over 24 h. Lipopolysaccharide (LPS; 300 ng/mL; 500 μ L) or the vehicle was added to the chambers, and the cells were cultured for an additional 24 h. GB123 (0.25 μ M) was added to the chambers for various incubation periods, and then the chambers were washed with phosphate-buffered saline (PBS) three times and stained with DAPI (1:1000) diluted in PBS. The cells were imaged by a Nikon motorized Ti2E confocal fluorescent microscope Ti2E with a Yokogawa W1 Spinning Disk (Olympus, Tokyo, Japan). The mean emission of the GB123 (Cy5 filter) intensity in cells was quantified by NIS Elements software package analysis (Nikon).

Accumulation Studies in Efflux Transporter-Overexpressing and Control Cells. Accumulation studies were conducted as we described before.³² Prior to the experiment, cells were incubated for 1 h with 1 mL of DMEM with 5 mM HEPES buffer, pH 7.3, in the presence or the absence of the P-gp inhibitor valsopodar (PSC-833; 1.65 μ M) or the vehicle (DMSO). After 1 h, the cells were further incubated for 1 h with 2 μ M GB123. Following three washes with ice-cold PBS, the cellular GB123 signal was measured at excitation/emission 620 nm/680 nm by a plate reader (Synergy HT, BioTek, Winooski, VT, USA). For MDCK-BCRP and MDCK-vector cells, experiments were conducted as described for MDCK-MDR1 cells, except that prior to the experiment cells were incubated with 1 mL of MEM with 5 mM HEPES, pH 7.3, in the presence or absence of 10 μ M fumitremorgin C (FTC). The studies were performed in triplicate on two separate days.

Cathepsin Binding in Transporter-Overexpressing and Control Cells. MDCK-MDR1, MDCK-CT, MDCK-BCRP, and MDCK-vector cells (3×10^6 cells/well) were seeded in 6-well plates. At 80% confluence, 1 μ M GB123 was added, and cells were incubated for 6 h. Cells were then washed with cold PBS and lysed using 60 μ L of RIPA buffer (50 mM Tris HCl, pH 7.4, 150 mM NaCl, 5 mM EDTA, 0.5% deoxycholate, and 0.1% SDS). The supernatant was collected after centrifugation for 5 min at 1200 rpm, 4 °C. Protein concentrations were determined by the BCA Protein Assay Reagent Kit. Total protein extracts (100 μ g) were separated by 10% acrylamide SDS-polyacrylamide gel electrophoresis (SDS-PAGE). Gels were scanned with a Typhoon FLA 9500 biomolecular imager (GE Healthcare Bio-Sciences AB, Uppsala, Sweden) at excitation/emission of 635 nm/670 nm. Proteins from the gels were transferred to nitrocellulose

membranes, which were blocked in Tris-buffered saline containing 0.1% Tween 20 (TBS-T) and 5% skim milk powder and probed overnight at 4 °C with the primary antibodies against β -actin (1:1,000), C219 (1:1000), and BXP-21 (1:250). The blots were then incubated with peroxidase-conjugated goat antirabbit secondary antibody or goat antimouse IgG at (1:10000) for 1 h and developed by enhanced chemiluminescence. The essays were repeated 5 times.

Animals. All animal experiment procedures were conducted in conformity with the Institutional Animal Care and Use Committee of The Hebrew University. (Protocols MD-18-5602-5 and MD-12-13360-5). Male C57BL/6J mice (6–8 weeks old, weighting 25–30 g), Balb-c mice (6–7 weeks old, weighting 20–25 g), and Wistar rats (175–200 g) were obtained from Harlan Laboratories, Rehovot, Israel. Animals were housed in temperature-controlled 21 °C and humidity-controlled 30–70% conditions with a 12 h light/dark cycle, with food and water provided.

Induction of Murine Chronic Epilepsy. We used the pilocarpine-induced model of chronic temporal lobe epilepsy, in which 2 h of pilocarpine-induced status epilepticus is known to result, after a relatively latent period of up to 8 weeks, in epileptogenesis (e.g., changes in the brain tissue that transform it to epileptic), most pronounced in the hippocampus.^{33,34} The epilepsy was induced in rats as we described before and in mice, by an adjusted protocol.³⁵ Briefly, mice were treated with intraperitoneal injections of pilocarpine in divided 10 mg/kg doses every 20 min, up to a maximum of 40 mg/(kg/mouse). Convulsions were terminated 2 h after their onset by intraperitoneal diazepam injection (10 mg/kg). The mice were hydrated by repeated subcutaneous saline and intraperitoneal glucose–saline injections. Experiments with the ABPs were conducted during the phase of chronic epilepsy, 8–9 weeks after status epilepticus.

Human Tissue. The study was approved by the Hadassah Medical Organization ethical review board (no. 0322-13-HMO) and patients, or their legal representatives, signed an informed consent prior to the surgery. Tissue collection was conducted as we described before,²² from patients who underwent epilepsy surgery.

One patient was a 19 year old male with focal seizures associated with a right lateral temporal vascular lesion, who used oxcarbazepine at the time of the surgery and has been almost seizure-free on a 7 year follow-up. He underwent lesionectomy and electrocorticography-guided resection of the adjacent epileptogenic tissue. The sample was taken from the anterior peri-lesional area. The second patient was an eight month old girl, with tuberous sclerosis, who was taking valproate, carbamazepine, and vigabatrin at the time of the surgery and was lost to follow-up thereafter. She underwent partial right frontal lobectomy, including excision of a frontomesial tuber. The sample was taken from the posterior part of the resected tissue.

Gel Electrophoresis Studies. Balb-c mice were treated intraperitoneally with 20 mg/kg of the cathepsin inhibitor GB111-NH₂ or the vehicle, three times, 96, 48, and 5 h before GB123 administration. GB123 was injected into the tail vein, 50 nmol/mouse. After 24 h they were anesthetized with isoflurane and sacrificed by cervical dislocation. Brain tissue was surgically excised and frozen in liquid nitrogen until analysis. Proteins were extracted by homogenizing tissue in 1.5 mL screw-cap tubes filled with stainless steel beads (Next

Advance Inc., SSB16) and RIPA buffer using a bead homogenizer (Bullet Blender Storm—BBY24M, Next Advance, NY, USA) at speed 8 for 3 min. Total protein extracts (120 μg) were separated by SDS-PAGE and visualized by scanning the gel with a Typhoon scanner FLA 9500 at excitation/emission wavelengths of 635 nm/670 nm (GE Healthcare Bio-Sciences AB, Uppsala, Sweden).

For the direct ex vivo analysis, the lysate proteins from mice not treated with GB111-NH₂ in vivo were incubated with either the cathepsin inhibitor GB111-NH₂ (5 μM) or the vehicle for 30 min, then with a fluorescent cathepsin activity-based probe, GB123 (2 μM), for 90 min. Equal protein amounts were separated by SDS-PAGE and scanned by the Typhoon scanner.

ABP Staining in Brain Slices. Mice were anesthetized with ketamine–xylazine 2% (100 mg/kg and 10 mg/kg intraperitoneal) and perfused with cold PBS. Brain tissue was excised and fixed with 4% paraformaldehyde (PFA) in PBS overnight, immersed for 7 days in 30% sucrose in PBS for cryoprotection, embedded in optimal cutting temperature (OCT) compound, and frozen at $-80\text{ }^{\circ}\text{C}$ until analysis. Brain sections (10 μM) were cut by a cryostat (Leica CM 1950 Cryostat, Wetzlar, Germany), incubated with 0.25 μM GB123 in DMEM for 3 h at $37\text{ }^{\circ}\text{C}$, and then washed overnight with PBS. Sections were blocked with 5% bovine serum albumin (BSA), 5% normal goat serum, and 0.1% triton for 1 h at room temperature for further histochemical labeling.

Rats were anesthetized using pentobarbital sodium (60 mg/kg, intraperitoneally), and their brains were harvested. Brain sections were prepared as described above and stained with 1 μM GB137 for 6 h at $37\text{ }^{\circ}\text{C}$. GB137 is a quenched cathepsin activity-based probe that binds active cathepsins B, L, and S, producing a very specific fluorescent signal with minimal background. Slides were submerged in 100% methanol for 6 min at $-20\text{ }^{\circ}\text{C}$, then washed with PBS, and covered with DAPI for microscopy.

Frozen human brain tissues were allowed to thaw slowly at room temperature; then they were embedded in OCT for sectioning and frozen again at $-80\text{ }^{\circ}\text{C}$ until analysis. Sections (10 μM) were cut by a cryostat and stained with GB137, like the rat brains.

Images ($1272.8 \times 1272.8\ \mu\text{m}^2$, magnification $\times 60$) were taken by a Nikon Ti2E confocal fluorescent microscope with a Yokogawa W1 spinning disk. The mean emission intensity of GB123 and GB137 at 630 nm/665 nm was quantified by the NIS Elements software package (Nikon).

In Vivo Imaging Studies. In vivo imaging was performed using an IVIS 200 imaging system (PerkinElmer, Waltham, MA, USA) with a Cy5.5 filter. Mice were shaved 1 day before the imaging. Anesthesia was induced in an induction chamber with isoflurane (2–3%); then the animals were placed in the imaging chamber and fitted with a nose cone connected to a vaporizer to maintain isoflurane (1.0–2.5%) flow. GB123, 50 nmol/(25 g mouse) (dissolved in 19% (v/v) dimethyl sulfoxide (DMSO) in sterile PBS) was administered into the tail vein. A naive mouse was treated with the vehicle as a control for background emission intensity. Mice were imaged at 1, 3, 6, and 24 h after GB123 injection. Body temperature was kept at $37\text{ }^{\circ}\text{C}$ using a heated platform. At the end of the imaging studies mice were sacrificed under anesthesia by ketamine (75 mg/kg, 70 μL /(20 g)) and xylazine (10 mg/kg). Blood samples were collected from the tail in heparinized 96-well plates. Brain, spleen, lungs, liver, heart, kidneys and gut

were collected and protected from light. Immediately thereafter, the organs were scanned ex vivo by the IVIS 200 imaging system.

Pharmacokinetic Analysis. The in vivo and ex vivo GB123 emission intensity was analyzed using Living Image (v4.7.3, PerkinElmer, Waltham, MA, USA).³² For comparison of the in vivo analysis of systemic GB123 kinetics, regions of interest (ROIs) were drawn over the two hind-limb feet (0.07 cm^2) and wells containing blood samples. The intensity of background emission (from vehicle-treated mice) was subtracted from each ROI. The emission intensity was quantified in radian efficiency units ([photons/second/steradian]/microwatt; [p/s/sr]/ μW). The area under the emission intensity–time curve (AUC) of GB123 was analyzed by using WinNonlin (v6.2, Pharsight, MountainView, CA, USA).

Histochemical Procedures. Brain slides were blocked with 5% bovine serum albumin (BSA) and 5% normal goat serum in 0.1% triton for 1 h at room temperature. The fixated tissue was incubated overnight with primary Iba1 (monocyte-like cells) or NeuN (neurons) antibodies at $4\text{ }^{\circ}\text{C}$. The slides were then washed three times with PBS, co-incubated for 1 h at room temperature with corresponding secondary antibody conjugated to Alexa 488 (for Iba1) (1:150) or Cy3 (for NeuN) (1:200), and covered with DAPI. Images were analyzed using the same microscopy method as described above for ex vivo staining of rats, human, and mice brain sections.

Statistical Analysis. The Mann–Whitney test or the Kruskal–Wallis test, as appropriate, were used for comparisons of sequential variables (Prism; GraphPad, La Jolla, CA, USA). Results are reported as the mean \pm SD, unless otherwise indicated. P value ≤ 0.05 was considered significant.

■ ASSOCIATED CONTENT

SI Supporting Information

The Supporting Information is available free of charge at <https://pubs.acs.org/doi/10.1021/acsomega.3c08759>.

Figure S1, showing IVIS-acquired systemic distribution of GB123 in mice; Figure S2, showing ex vivo hippocampal upload of GB123 in epileptic (also showed together with co-staining for myeloid cells or neurons in main Figure 5) compared with naive mice; Figure S3, showing DAPI-stained BV2 and RAW 264.7 cell images, obtained for background subtraction from the GB123 stained cultured (main Figure 6) (PDF)

■ AUTHOR INFORMATION

Corresponding Authors

Sara Eyal – *Institute for Drug Research, School of Pharmacy, The Hebrew University of Jerusalem, Jerusalem 9190501, Israel*; orcid.org/0000-0003-1275-6094; Phone: 972-2-675-7246; Email: sara.eyal@mail.huji.ac.il

Dana Ekstein – *Department of Neurology, the Agnes Ginges Center for Human Neurogenetics, Hadassah Medical Center, Jerusalem 9112001, Israel; Faculty of Medicine, The Hebrew University of Jerusalem, Jerusalem 9112102, Israel*; orcid.org/0000-0002-3860-6054; Email: dekstein@hadassah.org.il

Authors

Roa'a Hamed – Institute for Drug Research, School of Pharmacy, The Hebrew University of Jerusalem, Jerusalem 9190501, Israel

Emmanuelle Merquiol – Institute for Drug Research, School of Pharmacy, The Hebrew University of Jerusalem, Jerusalem 9190501, Israel

Ivan Zlotver – Institute for Drug Research, School of Pharmacy, The Hebrew University of Jerusalem, Jerusalem 9190501, Israel

Galia Blum – Institute for Drug Research, School of Pharmacy, The Hebrew University of Jerusalem, Jerusalem 9190501, Israel; orcid.org/0000-0002-9374-2489

Complete contact information is available at:

<https://pubs.acs.org/10.1021/acsomega.3c08759>

Author Contributions

[†]S.E. and D.E. have equal contribution as last authors. All authors provided substantial contributions to the conception or design of the work or the acquisition, analysis, or interpretation of data for the work; drafted the work or revised it critically for important intellectual content; and provided final approval of the version to be published.

Funding

The study was supported by Grant No. 60564 (cathepsin activity-based probes for diagnosing and treating epilepsy) awarded by the Kamin Program of Israel's Innovation Authority to G.B., S.E., and D.E.

Notes

The authors declare no competing financial interest.

[†]S.E. is a Dame Susan Garth Professor of Cancer Research and is affiliated with the David R. Bloom Centre for Pharmacy and the Adolf and Klara Brettler Centre for Research in Molecular Pharmacology and Therapeutics at The Hebrew University of Jerusalem, Israel.

ACKNOWLEDGMENTS

We are grateful to Prof. Qingcheng Mao (University of Washington) for providing the MDCK-vector and MDCK-BCRP cell lines and to Prof. Alfred Schinkel (The Netherlands Cancer Institute) for providing the MDCK and MDCK-MDR1 cell lines. We thank Prof. Boaz Tirosh (The Hebrew University) for providing the RAW 264.7 cell line and Prof. Sigal Fleisher-Berkovich (Ben-Gurion University, Israel) for providing the BV2 cell line. We thank Prof. Tamir Ben-Hur and Dr. Nina Fainstein for assisting with the histologic studies. We thank Dr. Emma Portnoy for epileptic rat brains. We are grateful to Drs. Mony Benifla and Odeya Bennet who cared for the patients whose tissues were used for the study and who obtained consent from patients to participate in the research.

ABBREVIATIONS USED:

ABC, adenosine triphosphate binding cassette; ABP, activity-based probes;; BBB, blood–brain barrier;; BCA, bicinchoninic acid;; FTC, fumitremorgin C; PFA, paraformaldehyde

REFERENCES

- (1) Kwan, P.; Brodie, M. J. Early identification of refractory epilepsy. *N. Engl. J. Med.* **2000**, *342*, 314–9.
- (2) Chen, Z.; Brodie, M. J.; Liew, D.; Kwan, P. Treatment Outcomes in Patients With Newly Diagnosed Epilepsy Treated With Established

and New Antiepileptic Drugs: A 30-Year Longitudinal Cohort Study. *JAMA Neurol.* **2018**, *75* (3), 279–86.

- (3) Han, H.; Mann, A.; Ekstein, D.; Eyal, S. Breaking bad: The structure and function of the blood-brain barrier in epilepsy. *AAPS J.* **2017**, *19*, 973–88.

- (4) Wickstrom, R.; Taraschenko, O.; Dilena, R.; Payne, E. T.; Specchio, N.; Nabhout, R.; et al. International consensus recommendations for management of New Onset Refractory Status Epilepticus (NORSE) including Febrile Infection-Related Epilepsy Syndrome (FIRES): Summary and Clinical Tools. *Epilepsia* **2022**, *63* (11), 2827–2839.

- (5) French, J. A.; Cole, A. J.; Faught, E.; Theodore, W. H.; Vezzani, A.; Liow, K.; et al. Safety and Efficacy of Natalizumab as Adjunctive Therapy for People With Drug-Resistant Epilepsy: A Phase 2 Study. *Neurology* **2021**, *97* (18), e1757–e1767.

- (6) Kaminski, R. M.; Rogawski, M. A.; Klitgaard, H. The Potential of Antiseizure Drugs and Agents that Act on Novel Molecular Targets as Antiepileptogenic Treatments. *Neurotherapeutics* **2014**, *11* (2), 385–400.

- (7) Hook, G.; Reinheckel, T.; Ni, J.; Wu, Z.; Kindy, M.; Peters, C.; et al. Cathepsin B Gene Knockout Improves Behavioral Deficits and Reduces Pathology in Models of Neurologic Disorders. *Pharmacol. Rev.* **2022**, *74* (3), 600.

- (8) Salpeter, S. J.; Pozniak, Y.; Merquiol, E.; Ben-Nun, Y.; Geiger, T.; Blum, G. A Novel Cysteine Cathepsin Inhibitor Yields Macrophage Cell Death and Mammary Tumor Regression. *Oncogene* **2015**, *34*, 6066–78.

- (9) Abd-Elrahman, I.; Kosuge, H.; Wisnes Sadan, T.; Ben-Nun, Y.; Meir, K.; Rubinstein, C.; Bogoy, M.; McConnell, M. V.; Blum, G. Cathepsin Activity-Based Probes and Inhibitor for Preclinical Atherosclerosis Imaging and Macrophage Depletion. *PLoS One* **2016**, *11*, No. e0160522.

- (10) Ben-Aderet, L.; Merquiol, E.; Fahham, D.; Kumar, A.; Reich, E.; Ben-Nun, Y.; et al. Detecting cathepsin activity in human osteoarthritis via activity-based probes. *Arthritis Res. Ther.* **2015**, *17* (1), 69.

- (11) Weiss-Sadan, T.; Ben-Nun, Y.; Maimoun, D.; Merquiol, E.; Abd-Elrahman, I.; Gotsman, I.; et al. A Theranostic Cathepsin Activity-Based Probe for Noninvasive Intervention in Cardiovascular Diseases. *Theranostics* **2019**, *9* (20), 5731–8.

- (12) Nakanishi, H. Neuronal and microglial cathepsins in aging and age-related diseases. *Ageing Res. Rev.* **2003**, *2* (4), 367–81.

- (13) Kingham, P. J.; Pocock, J. M. Microglial secreted cathepsin B induces neuronal apoptosis. *J. Neurochem.* **2001**, *76* (5), 1475–84.

- (14) Houseweart, M. K.; Pennacchio, L. A.; Vilaythong, A.; Peters, C.; Noebels, J. L.; Myers, R. M. Cathepsin B but not cathepsins L or S contributes to the pathogenesis of Unverricht-Lundborg progressive myoclonus epilepsy (EPM1). *J. Neurobiol.* **2003**, *56* (4), 315–27.

- (15) Rinne, R.; Saukko, P.; Järvinen, M.; Lehesjoki, A.-E. Reduced cystatin B activity correlates with enhanced cathepsin activity in progressive myoclonus epilepsy. *Ann. Med.* **2002**, *34* (5), 380–5.

- (16) Akahoshi, N.; Murashima, Y. L.; Himi, T.; Ishizaki, Y.; Ishii, I. Increased expression of the lysosomal protease cathepsin S in hippocampal microglia following kainate-induced seizures. *Neurosci. Lett.* **2007**, *429* (2–3), 136–141.

- (17) Banerjee, M.; Sasse, V. A.; Wang, Y.; Maulik, M.; KAR, S. Increased levels and activity of cathepsins B and D in kainate-induced toxicity. *Neuroscience* **2015**, *284*, 360–373.

- (18) Ben-Nun, Y.; Merquiol, E.; Brandis, A.; Turk, B.; Scherz, A.; Blum, G. Photodynamic quenched cathepsin activity based probes for cancer detection and macrophage targeted therapy. *Theranostics* **2015**, *5* (8), 847–62.

- (19) Blum, G.; Mullins, S. R.; Keren, K.; Fonovic, M.; Jedeszko, C.; Rice, M. J.; et al. Dynamic imaging of protease activity with fluorescently quenched activity-based probes. *Nat. Chem. Biol.* **2005**, *1* (4), 203–9.

- (20) Blum, G.; von Degenfeld, G.; Merchant, M. J.; Blau, H. M.; Bogoy, M. Noninvasive optical imaging of cysteine protease activity using fluorescently quenched activity-based probes. *Nat. Chem. Biol.* **2007**, *3* (10), 668–77.

- (21) Eyal, S.; Hsiao, P.; Unadkat, J. D. Drug interactions at the blood-brain barrier: fact or fantasy? *Pharmacol Ther* **2009**, *123*, 80–10.
- (22) Brukner, A. M.; Billington, S.; Benifla, M.; Nguyen, T. B.; Han, H.; Bennett, O.; et al. Abundance of P-glycoprotein and Breast Cancer Resistance Protein Measured by Targeted Proteomics in Human Epileptogenic Brain Tissue. *Mol. Pharmaceutics* **2021**, *18* (6), 2263–73.
- (23) U.S. Food and Drug Administration (FDA). *Development and Drug Interactions: Table of Substrates, Inhibitors and Inducers*, March 10, 2020. <https://www.fda.gov/drugs/drug-interactions-labeling/drug-development-and-drug-interactions-table-substrates-inhibitors-and-inducers> (accessed 2022-01-21).
- (24) Ravizza, T.; Gagliardi, B.; Noé, F.; Boer, K.; Aronica, E.; Vezzani, A. Innate and adaptive immunity during epileptogenesis and spontaneous seizures: Evidence from experimental models and human temporal lobe epilepsy. *Neurobiol. Dis.* **2008**, *29* (1), 142–60.
- (25) Varvel, N. H.; Neher, J. J.; Bosch, A.; Wang, W.; Ransohoff, R. M.; Miller, R. J.; Dingleline, R. Infiltrating monocytes promote brain inflammation and exacerbate neuronal damage after status epilepticus. *Proc. Natl. Acad. Sci. U. S. A.* **2016**, *113*, E5665–E5674.
- (26) Ravizza, T.; Gagliardi, B.; Noé, F.; Boer, K.; Aronica, E.; Vezzani, A. Innate and adaptive immunity during epileptogenesis and spontaneous seizures: evidence from experimental models and human temporal lobe epilepsy. *Neurobiol. Dis.* **2008**, *29*, 142–60.
- (27) Hamed, R.; Eyal, A. D.; Berman, E.; Eyal, S. In silico screening for clinical efficacy of antiseizure medications: Not all central nervous system drugs are alike. *Epilepsia* **2023**, *64* (2), 311–9.
- (28) Yoon, M. C.; Solania, A.; Jiang, Z.; Christy, M. P.; Podvin, S.; Mosier, C.; Lietz, C. B.; Ito, G.; Gerwick, W. H.; Wolan, D. W.; et al. Selective Neutral pH Inhibitor of Cathepsin B Designed Based on Cleavage Preferences at Cytosolic and Lysosomal pH Conditions. *ACS Chem. Biol.* **2021**, *16* (9), 1628–1643.
- (29) Wang, Y.; Gao, A.; Xu, X.; Dang, B.; You, W.; Li, H.; Yu, Z.; Chen, G. The neuroprotection of lysosomotropic agents in experimental subarachnoid hemorrhage probably involving the apoptosis pathway triggering by cathepsins via chelating intralysosomal iron. *Mol. Neurobiol.* **2015**, *52*, 64–77.
- (30) Hook, G.; Kindy, M.; Hook, V. J. Cathepsin B Deficiency Improves Memory Deficits and Reduces Amyloid- β in hA β PP Mouse Models Representing the Major Sporadic Alzheimer's Disease Condition. *J. Alzheimer's Dis.* **2023**, *93* (1), 33–46.
- (31) Kim, K. R.; Cho, E. J.; Eom, J. W.; Oh, S. S.; Nakamura, T.; Oh, C. K.; Lipton, S. A.; Kim, Y. H. S-Nitrosylation of cathepsin B affects autophagic flux and accumulation of protein aggregates in neurodegenerative disorders. *Cell Death Differ.* **2022**, *29* (11), 2137–2150.
- (32) Portnoy, E.; Gurina, M.; Magdassi, S.; Eyal, S. Evaluation of the near infrared compound indocyanine green as a probe substrate of P-glycoprotein. *Mol. Pharmaceutics* **2012**, *9*, 3595–601.
- (33) Gröticke, I.; Hoffmann, K.; Löscher, W. Behavioral alterations in the pilocarpine model of temporal lobe epilepsy in mice. *Exp. Neurol.* **2007**, *207* (2), 329–349.
- (34) Glien, M.; Brandt, C.; Potschka, H.; Voigt, H.; Ebert, U.; Löscher, W. Repeated low-dose treatment of rats with pilocarpine: Low mortality but high proportion of rats developing epilepsy. *Epilepsy Res.* **2001**, *46* (2), 111–119.
- (35) Portnoy, E.; Polyak, B.; Inbar, D.; Kenan, G.; Rai, A.; Wehrli, S. L.; Eyal, S. Tracking inflammation in the epileptic rat brain by bifunctional fluorescent and magnetic nanoparticles. *Nanomed.: Nanotechnol., Biol. Med.* **2016**, *12* (5), 1335–1345.